

The official journal of

INTERNATIONAL FEDERATION OF PIGMENT CELL SOCIETIES · SOCIETY FOR MELANOMA RESEARCH

PIGMENT CELL & MELANOMA Research

Cooperative induction of apoptosis in NRAS mutant melanoma by inhibition of MEK and ROCK

Celia J. Vogel, Marjon A. Smit, Gianluca Maddalo, Patricia A. Possik, Rolf W. Sparidans, Sjoerd H. van der Burg, Els M. Verdegaal, Albert J. R. Heck, Ahmed A. Samatar, Jos H. Beijnen, A. F. Maarten Altelaar and Daniel S. Peeper

DOI: [10.1111/pcmr.12364](https://doi.org/10.1111/pcmr.12364)

Volume 28, Issue 3, Pages 307–317

If you wish to order reprints of this article, please see the guidelines [here](#)

Supporting Information for this article is freely available [here](#)

EMAIL ALERTS

Receive free email alerts and stay up-to-date on what is published in Pigment Cell & Melanoma Research – [click here](#)

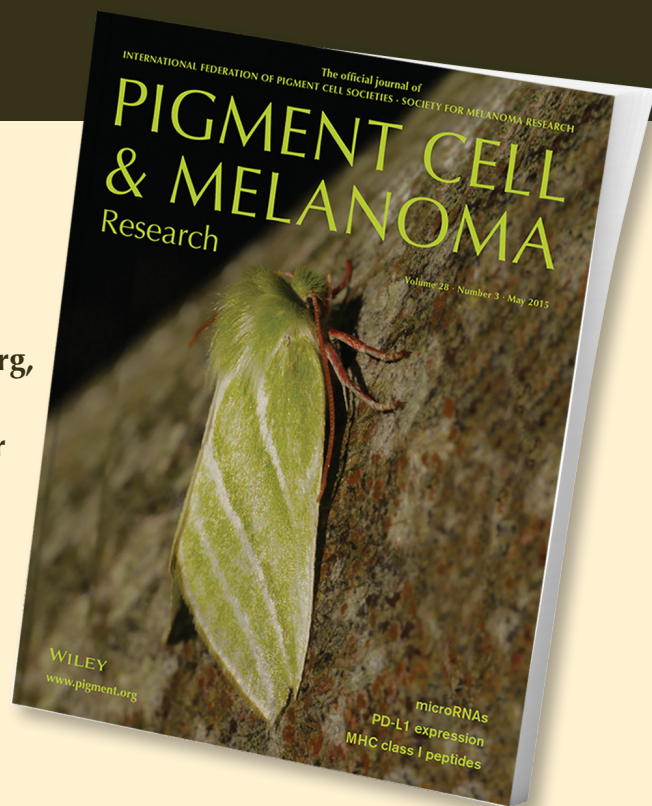
Submit your next paper to PCMR online at <http://mc.manuscriptcentral.com/pcmr>

Subscribe to PCMR and stay up-to-date with the only journal committed to publishing basic research in melanoma and pigment cell biology

As a member of the IFPCS or the SMR you automatically get online access to PCMR. Sign up as a member today at www.ifpcs.org or at www.societymelanomaresarch.org

To take out a personal subscription, please [click here](#)

More information about Pigment Cell & Melanoma Research at www.pigment.org



Cooperative induction of apoptosis in NRAS mutant melanoma by inhibition of MEK and ROCK

Celia J. Vogel^{1,‡}, Marjon A. Smit^{1,†,‡}, Gianluca Maddalo^{2,3}, Patricia A. Possik¹, Rolf W. Sparidans⁴, Sjoerd H. van der Burg⁵, Els M. Verdegaal⁵, Albert J. R. Heck^{2,6}, Ahmed A. Samatar⁷, Jos H. Beijnen⁸, A. F. Maarten Altelaar^{2,6} and Daniel S. Peeper¹

1 Division of Molecular Oncology, The Netherlands Cancer Institute, Amsterdam, The Netherlands **2** Biomolecular Mass Spectrometry & Proteomics, Utrecht Institute for Pharmaceutical Sciences and Bijvoet Center for Biomolecular Research, Utrecht University, Utrecht, The Netherlands **3** Center for Biomembrane Research, Department of Biochemistry and Biophysics, Stockholm University, Stockholm, Sweden **4** Division of Pharmacoepidemiology and Clinical Pharmacology, Department of Pharmaceutical Sciences, Utrecht University, Utrecht, The Netherlands **5** Department of Clinical Oncology, Leiden University Medical Center, Leiden, The Netherlands **6** Netherlands Proteomics Centre, Utrecht, The Netherlands **7** TheraMet Biosciences, Princeton Junction, NJ, USA **8** Department of Pharmacy and Pharmacology, Slotervaart Hospital, Amsterdam, The Netherlands

‡Current address: Department of Medical Genetics, Institute of Human Genetics, Tübingen University, Tübingen, Germany

CORRESPONDENCE Daniel S. Peeper, e-mail: d.peeper@nki.nl

‡These authors contributed equally to this work.

KEYWORDS NRAS/melanoma/ROCK/MEK/targeted therapy

PUBLICATION DATA Received 24 March 2014, revised and accepted for publication 25 February 2015, published online 28 February 2015

doi: 10.1111/pcmr.12364

Summary

No effective targeted therapy is currently available for NRAS mutant melanoma. Experimental MEK inhibition is rather toxic and has only limited efficacy in clinical trials. At least in part, this is caused by the emergence of drug resistance, which is commonly seen for single agent treatment and shortens clinical responses. Therefore, there is a dire need to identify effective companion drug targets for NRAS mutant melanoma. Here, we show that at concentrations where single drugs had little effect, ROCK inhibitors GSK269962A or Fasudil, in combination with either MEK inhibitor GSK1120212 (Trametinib) or ERK inhibitor SCH772984 cooperatively caused proliferation inhibition and cell death in vitro. Simultaneous inhibition of MEK and ROCK caused induction of Bim_{EL}, PARP, and Puma, and hence apoptosis. In vivo, MEK and ROCK inhibition suppressed growth of established tumors. Our findings warrant clinical investigation of the effectiveness of combinatorial targeting of MAPK/ERK and ROCK in NRAS mutant melanoma.

Introduction

The RAS/RAF/MEK/ERK (MAPK/ERK) pathway is frequently used by melanomas to gain growth, survival, and other cancer-relevant properties (Fedorenko et al.,

2013) and is activated in 90% of cutaneous melanomas, with ~50% carrying a BRAF codon 600 mutation and another ~20% carrying a NRAS codon 61 mutation (Eggermont et al., 2014). The latter cannot be treated with BRAF mutation-specific drugs such as Vemurafenib

Significance

Whereas the perspectives for patients with BRAF^{V600E} melanoma have significantly improved thanks to targeted therapies inhibiting the MAPK/ERK pathway, there has been no such development for mutant NRAS, which drives up to a quarter of all melanomas. We uncovered an unexpected cooperative induction of apoptosis by simultaneous pharmacologic inhibition of either MEK or ERK together with ROCK in vitro and suppression of tumor growth by MEK and ROCK inhibition. This study merits clinical validation, to meet a dire need of patients with NRAS mutant melanoma.

and Dabrafenib, which have improved melanoma therapy greatly after a long impasse (Chapman et al., 2011; Hauschild et al., 2012). As inhibitors of RAS isoforms are particularly hard to develop (Fedorenko et al., 2013; Ji et al., 2012; Ostrem et al., 2014), inhibitors of downstream kinases MEK [GSK1120212/Trametinib (Gilmartin et al., 2011)] and ERK [SCH772984 (Morris et al., 2013), VTX11-e (Aronov et al., 2009)] are being explored instead. NRAS mutant melanomas are currently treated with classical chemotherapy, emerging immunotherapies, and MEK inhibitors, but the latter are used only experimentally and toxicity is an issue (Ascierto et al., 2013). Furthermore, as is commonly seen for single agent treatments, the emergence of drug resistance limits responses (Diaz et al., 2012) and effects of MEK inhibitors are even more short lived than for BRAF inhibitors (Ascierto et al., 2013). Therefore, it is imperative to identify effective (companion) drug targets for NRAS melanoma.

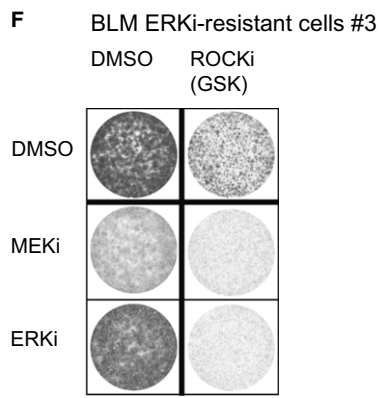
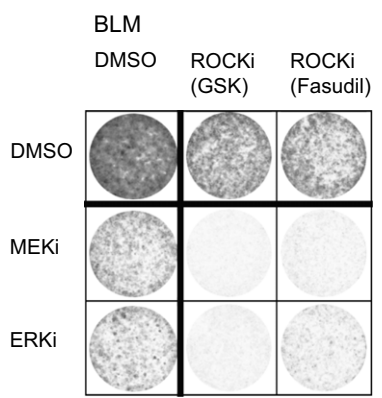
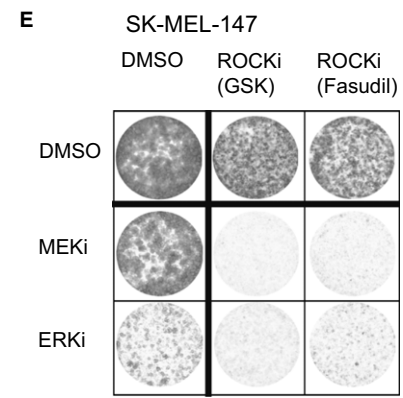
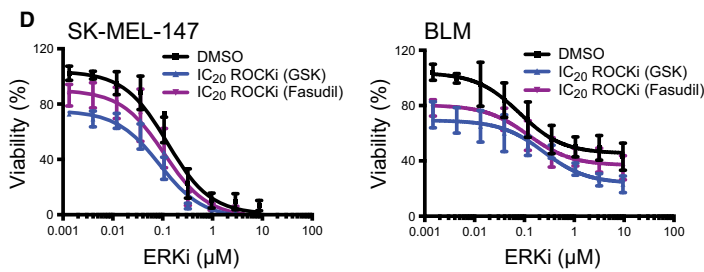
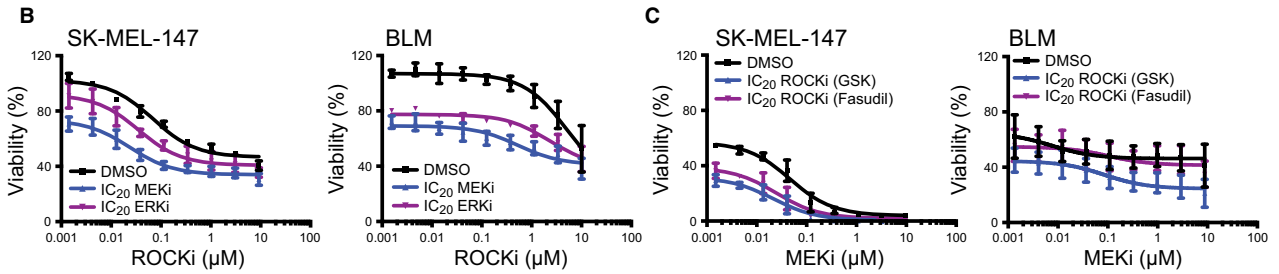
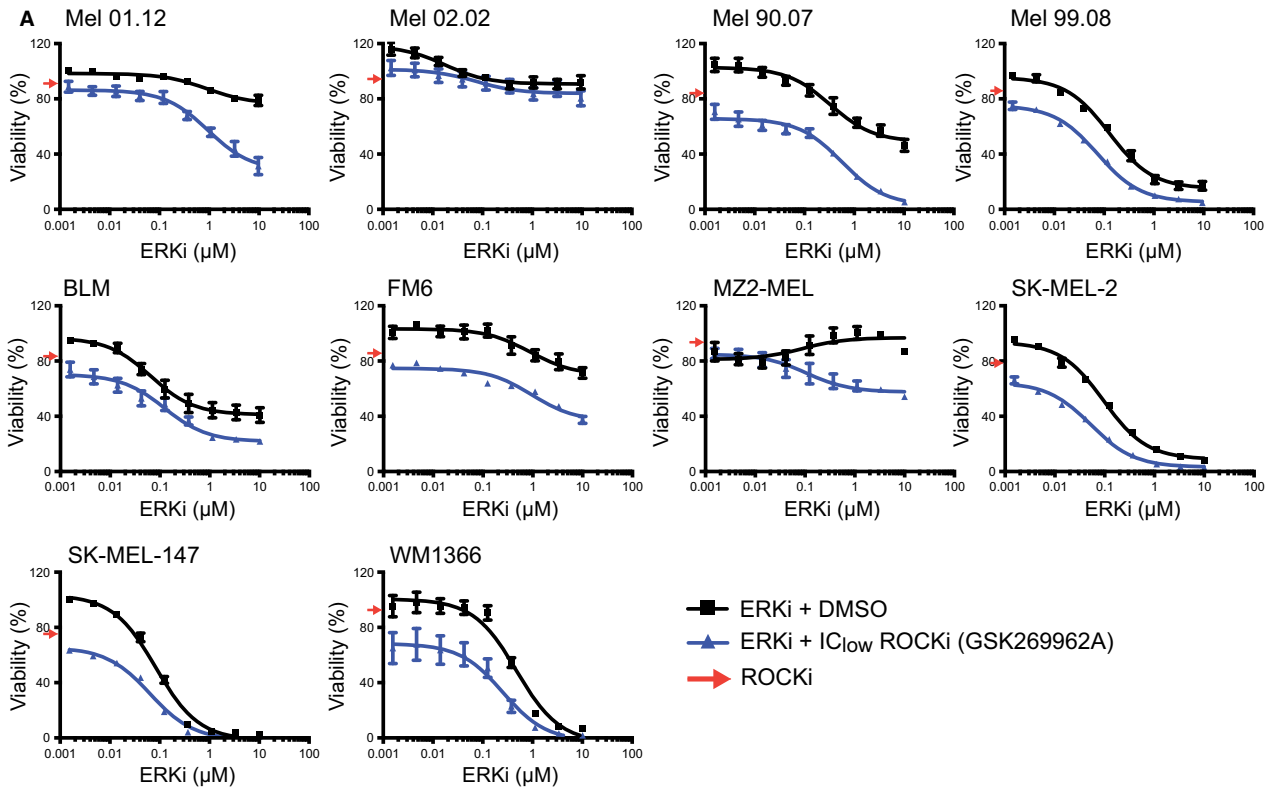
ROCK1 and 2 are highly homologous Rho GTPase-activated serine/threonine kinases with an overlapping substrate spectrum including cytoskeletal proteins, thus regulating migration, invasion, and metastasis (Amano et al., 2010). Consequently, most research into ROCK inhibition as cancer therapy has focused on the suppression of metastasis (Nakajima et al., 2003). However, ROCK1 and 2 have also been implicated in tumor cell proliferation and/or survival (Street and Bryan, 2011). ROCK inhibitors as single agents have been shown to suppress primary tumor growth of a grafted murine melanoma cell line without BRAF or NRAS mutations (Routhier et al., 2010) and in a genetic mouse model for breast cancer (Patel et al., 2012). To improve the limited and heterogeneous responses observed, it has been proposed to combine ROCK inhibitors with chemotherapy, irradiation, or targeted agents (Rath and Olson, 2012; Routhier et al., 2010). Overall, the impact of ROCK inhibition on proliferation and survival of melanoma upon exposure to targeted therapies such as MAPK/ERK pathway inhibitors has been underexplored. Therefore, we decided to investigate ROCK as a combination target for the treatment of NRAS mutant melanoma with MAPK/ERK pathway inhibitors.

Results

NRAS mutant melanoma cells are sensitive to combinatorial inhibition of MAPK/ERK and ROCK pathways

We first determined the sensitivity of a panel of NRAS mutant melanoma cell lines to targeted inhibitors as single agents. We observed a wide spectrum of sensitivities to ERK or MEK inhibitors (designated ERKi for SCH772984 and MEKi for GSK1120212 from now on) as expected, due to the pleiotropic nature of RAS signaling (Karnoub and Weinberg, 2008) and the high number of genetic alterations typical for melanoma (Walia et al., 2012). Some cell lines were exquisitely sensitive to ERK or MEK inhibitors (e.g. Mel 99.08, SK-MEL-147), while others were intermediately or hardly sensitive, indicative of intrinsic resistance (e.g. Mel 90.07, Mel 02.02, respectively), displaying a large residual population of cells even at the highest inhibitor doses (Figure 1A and Figure S1A, black curves). While ROCK inhibitor GSK269962A (ROCKi) showed only modest activity as single agent (Figure 1B and Figure S1B, black curves), when used only at a low inhibitory concentration in combination with ERK or MEK inhibition, it reduced viability of almost all NRAS mutant cell lines examined (Figure 1A and Figure S1A, blue curves). The reverse was also true: low inhibitory concentrations of ERKi or MEKi combined with ROCKi reduced viability in most cell lines (Figure 1B and Figure S1B). ROCK inhibitors GSK269962A and Fasudil had similar effects in all assays (Figure 1C–E). Whereas GSK269962A is not currently in clinical use, the less specific and chemically unrelated ROCK inhibitor Fasudil is used to treat cardiovascular diseases (Rath and Olson, 2012) and could be repurposed. We observed a cooperative effect of ROCK and MEK or ERK inhibition (Figure 1E) in long-term proliferation assays, for which we titrated the individual inhibitor concentrations to have little effect on their own. Furthermore, the combination of ERKi or MEKi with ROCKi was effective in NRAS mutant melanoma sublines, which were made resistant to ERKi by long-term culture in 1 μ M of the inhibitor (Figure 1F and Figure S2A). These resistant lines show downstream MAPK/ERK pathway activation in the presence of ERKi (Figure S2B). Taken together, these results demonstrate that simultaneous

Figure 1. NRAS mutant melanoma cells are sensitive to combinatorial inhibition of MAPK/ERK and ROCK pathways. (A–D) NRAS mutant melanoma cell lines as indicated in the panels. Cells were treated for 72 h with inhibitors diluted in threefold steps from 10 μ M to 1.5 nM: ROCK inhibitor GSK269962A was combined with cell line-specific low inhibitory concentrations (IC_{low}) of MEKi (blue, B), or ERKi (purple, B); ERKi or MEKi were combined with cell line-specific low inhibitory concentrations (IC_{low}) of ROCK inhibitors (GSK269962A, blue, A, C, D, or Fasudil, purple, C, D). Cell viability was determined with CellTiter Blue. Inhibitor concentrations are depicted on the x-axis and the percentage of viable cells on the y-axis. Curves are average values of at least three independent experiments. Error bars represent the SEM for all panels. The red arrowheads indicate reduced cell viability by treatment with ROCKi as single agent. (E) SK-MEL-147 and BLM cells were treated for 7 days with DMSO, inhibitors of MEK, ERK, or ROCK (GSK269962A, Fasudil) and stained with crystal violet. One representative experiment of five independent experiments is shown. (F) An ERK inhibitor-resistant subline of BLM cells was treated for 7 days with DMSO, inhibitors of MEK, ERK, or ROCK (GSK269962A) and stained with crystal violet. One representative experiment of three independent experiments is shown.



inhibition of MEK/ERK and ROCK signaling reduced viability of NRAS mutant melanoma cells in a cooperative fashion both short and long term and in both treatment-naïve and ERKi-resistant cell lines.

ROCK and MEK or ERK inhibitors cooperatively induce apoptosis and cytostasis

To investigate how inhibitors of MEK or ERK in combination with ROCK inhibitors cooperate to influence signaling and cell viability in NRAS mutant melanoma, we first compared samples of the highly sensitive SK-

MEL-147 cell line upon treatment with MEKi/ERKi, ROCKi, or both. MEK and ERK inhibitors altered transcript levels of established MEK target genes in agreement with publications from other groups (Dry et al., 2010; Packer et al., 2009): while ELF1 was upregulated, ETV5 and PHLDA1 were downregulated (Figure S3A). MEK inhibition reduced phosphorylation of ERK1/2 and their direct downstream target p90RSK1 to undetectable levels indicating efficient MAPK/ERK pathway inhibition (Figure 2A). ERK inhibition reduced phosphorylated p90RSK1 to undetectable levels as well (Figure S3B).

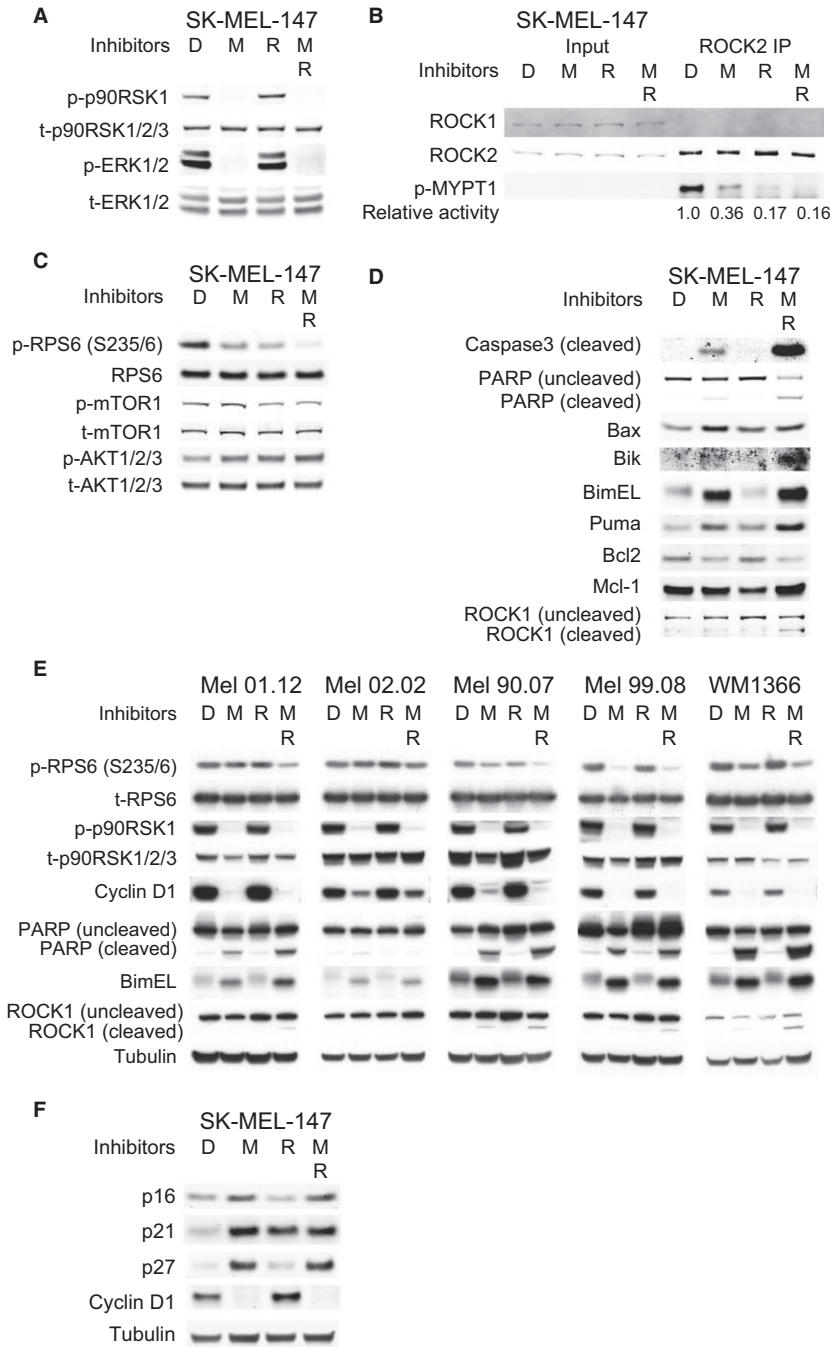


Figure 2. ROCK and MEK inhibitors cooperatively induce apoptosis and cytostasis. NRAS mutant melanoma cell lines as indicated in the panels were treated for 24 h with DMSO (= D), MEKi (= M, 0.1 μM), ROCK inhibitor GSK269962A (= R, 1 μM), or both. Adherent and floating cells were harvested, lysed with the appropriate buffers and used for immunoblotting for the indicated processes and proteins (A–F) and ROCK2 kinase assays (B). (A–F) Immunoblot detection of A: MAPK/ERK signaling; B: ROCK2 kinase assay on recombinant substrate MYPT1 and relative kinase activity; C: RPS6, AKT, mTOR; D: Pro- and anti-apoptotic signaling; E: RPS6, p90RSK, Cyclin D1, PARP, Bim, ROCK1; F: Cell cycle regulators. One representative experiment of three independent experiments is shown (A–F).

These effects on MAPK/ERK signaling were not seen for ROCK inhibition (Figure 2A and Figure S3B).

As ROCK signaling branches into many downstream substrates, we determined the activity of ROCK kinase. Its activity was reduced by ROCKi single treatment and in combination with MEKi (Figure 2B, lanes R and MR), and some reduction was also observed upon treatment with MEKi (Figure 2B, lane M). While phosphorylation of 40S ribosomal protein S6 (RPS6) was decreased by single treatment with MEKi or ROCKi, this effect was enhanced by the combination (Figure 2C). Five of seven cell lines examined showed reduced levels of phosphorylated RPS6 in MEKi-ROCKi cotreated samples (Figure 2E and Figure S3B). This was also observed when combining ROCK inhibition with ERK inhibition (Figure S3B). Although RPS6 acts not only downstream of the MAPK/ERK pathway, but also the PI₃K pathway (Mendoza et al., 2011), we did not observe deregulation of p-AKT or p-mTOR (Figure 2C).

ROCK inhibition did lead to increased induction of pro-apoptotic signaling by MEKi. While the levels of the pro-apoptotic proteins cleaved caspase 3, cleaved PARP, unphosphorylated Bim_{EL}, Bik, and Puma increased by single treatment with MEKi, this effect was further increased in samples treated with MEKi and ROCKi. Along those lines, while the levels of the anti-apoptotic protein Bcl2 decreased by MEKi, Bcl2 levels were further decreased by the combination of MEKi and ROCKi (Figure 2D). *BIM* transcripts were induced by MEKi, but not increased further by adding ROCKi, while ROCKi alone did not induce the transcripts at all (Figure S3C), suggesting that the further increase in Bim_{EL} protein levels by MEKi-ROCKi cotreatment occurs by post-transcriptional mechanisms. The effects on PARP, Bim_{EL}, and ROCK1 were seen across several NRAS mutant melanoma cell lines and for either MEKi or ERKi in combination with ROCKi (Figure 2E and Figure S3D). Increased levels of apoptosis coincided with the appearance of a ~130 kDa ROCK1 cleavage fragment (Figure 2D, lane M+R), which is likely the result of caspase 3 activation (Sebbagh et al., 2001). MEKi treatment also increased the abundance of cell cycle inhibitors p16^{INK4A}, p21^{CIP1}, and p27^{KIP1} and abolished the levels of cell cycle progression protein Cyclin D1 (Figure 2F). p21^{CIP1} was upregulated in ROCKi-treated samples as expected (Sahai et al., 2001), but its levels did not increase further in the cotreated samples. Of note, most cotreated NRAS mutant melanoma cell lines displayed both apoptotic and cytostatic responses, and the effects on PARP, Bim_{EL}, and ERK signaling were observed both for attached and a mixture of attached plus floating cells (Figure S4A).

To gain a more comprehensive view of changes in protein signaling induced by inhibition of MEK, ROCK, or both, we performed a mass spectrometry-based (phospho)proteomics approach (Figure S4B; Altelaar et al., 2013). The analysis focused on those proteins that significantly changed their expression or phosphorylation

levels and followed the same pattern in single and combination inhibitor treatments (Figure S5A,B, and Table S1). We merged the data of these proteins and used the DAVID tool for functional annotation clustering (Table S2). Seven of the 18 clusters had an enrichment score above 1.3, which is equivalent to a $P < 0.05$, including processes related to DNA replication and mitosis (Figure 3A). Of note, we used IC₂₀ concentrations of the drugs, to avoid secondary effects related to cell death. Therefore, apoptotic signaling proteins just failed to reach statistical significance.

The volcano plots of whole proteome analyses compare protein levels between pairs of samples with different treatments. Individual proteins that changed significantly by single treatment with MEKi or ROCKi and with the combination of both inhibitors are shown. Of those, we displayed only the proteins whose changes in levels followed the same trend across single and combined inhibitor treatments; they were concordantly regulated. Treatment with either MEKi, ROCKi, or MEKi plus ROCKi led to downregulation of RACGAP1, UBE2T, and UHRF1 levels, whereas the levels of ATP2B4, NGFR, and SORBS2 were upregulated (Figure 3B). Combined inhibitor treatment had a greater effect on the levels of those proteins than single inhibitor treatment did (Figure S5B). Our analysis showed that single or combined copy-number alterations, mutations, changes in mRNA, or (phospho)protein levels occur with higher frequencies per gene in melanomas with NRAS than BRAF mutations, except for UBE2T (Figure 3C and Table S3). Furthermore, analysis of 44 cancer datasets revealed that the set of the six genes is affected in more than 20% of pancreatic, melanoma, breast, uterine, liver, lung, ovarian, and stomach cancer samples (Figure S6 and Table S4). Taken together, inhibition of the MAPK/ERK and ROCK pathways influences cellular processes cooperatively, in particular apoptosis and proliferation (DNA replication and mitosis) in NRAS mutant melanoma cells. These results are in line with the cytostatic and cytotoxic effects observed in vitro by cotreatment of NRAS mutant melanoma cell lines with MAPK/ERK and ROCK inhibitors.

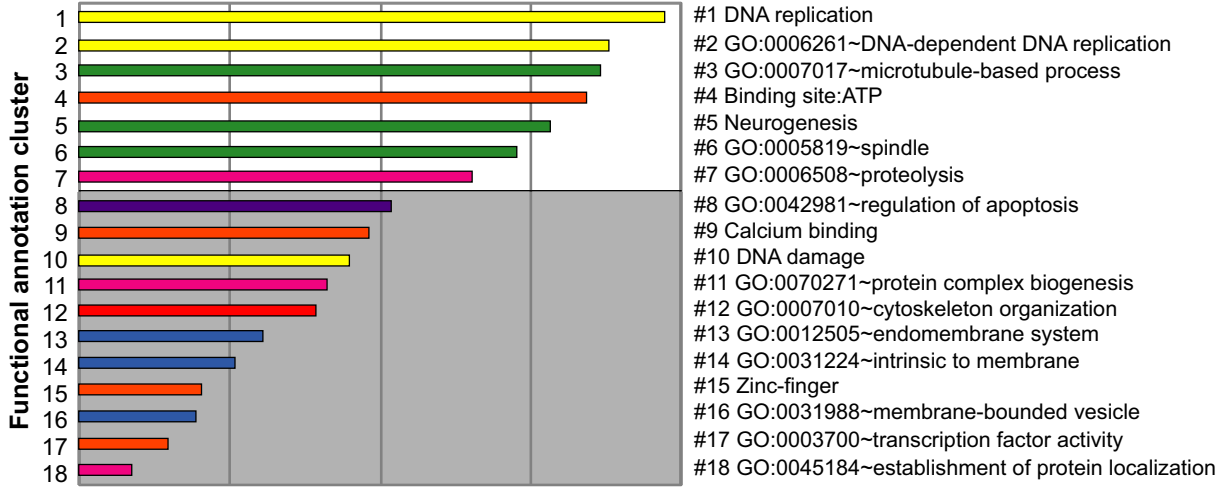
NRAS mutant melanoma is sensitive to the combined inhibition of MEK and ROCK in vivo

Our in vitro results prompted the question whether the combined inhibition of MEK and ROCK would also inhibit melanoma growth in vivo. We injected SK-MEL-147 cells subcutaneously into immunocompromised mice. To approximate the situation in the clinic, we treated established tumors at a size of up to 150 mm³ and observed moderate inhibition of tumor growth for single drug treatments at a dose of 0.05 mg/kg of MEKi or 10 mg/kg of ROCKi. Importantly, the combination treatment with ROCK and MEK inhibitors at these doses strongly suppressed tumor growth (Figure 4A). The mice from single agent-treated groups had to be sacrificed

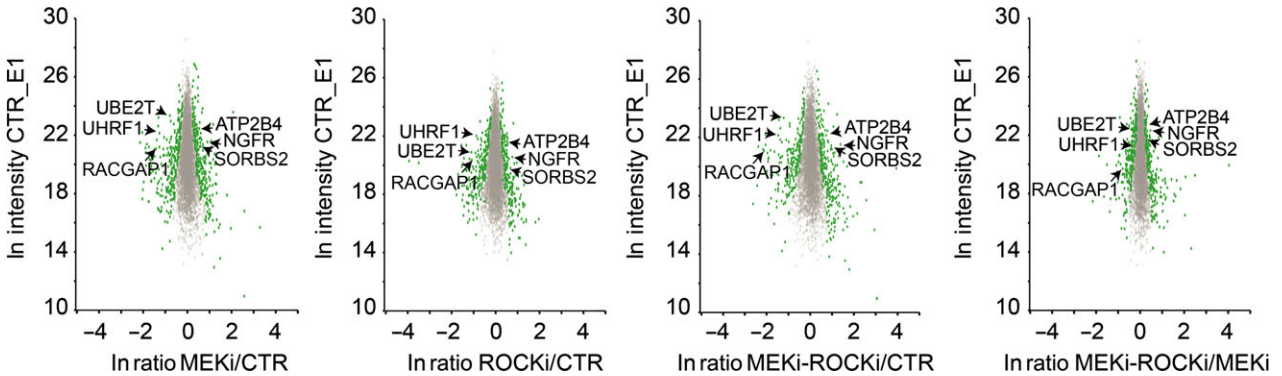
- A**
- DNA replication and damage
 - Microtubule-dependent processes
 - ATP-binding, calcium-binding, zinc-finger, transcription factor activity
 - Protein regulation
 - Cytoskeleton
 - Membrane-related processes
 - Regulation of apoptosis

Enrichment score

0.00 0.50 1.00 1.50 2.00



B



C

	All samples	BRAF MT	NRAS MT	BRAF/NRAS MT	BRAF/NRAS WT	Alteration frequency
Number of samples	477	177	92	27	181	100%
BRAF	43%	100%	0%	100%	0%	90%
NRAS	25%	0%	100%	100%	0%	80%
ATP2B4	20%	20%	27%	37%	14%	70%
NGFR	9%	8%	10%	22%	7%	60%
RACGAP1	6%	6%	12%	15%	3%	50%
SORBS2	9%	8%	15%	7%	6%	40%
UBE2T	15%	14%	14%	22%	17%	30%
UHRF1	5%	4%	9%	11%	4%	20%
						10%
						0%

Figure 3. ROCK and MEK inhibitors cooperatively alter the proteome. SK-MEL-147 cells were treated for 24 h with DMSO (= D), MEKi (= M, 0.02 μ M), ROCK inhibitor GSK269962A (= R, 1 μ M), or both. Adherent and floating cells were harvested, lysed with the appropriate buffers and analyzed by mass spectrometry. (A) DAVID pathway analysis of proteins that significantly changed their expression levels or phosphorylation levels and followed the same trend in all treated samples across two independent experiments. Clusters above the gray field have an enrichment score >1.3 (equivalent to a $P < 0.05$). (B) Ratio versus intensity plots of the whole proteome analyses for selected significant entries shown in the heat map in Figure S5B. Entries with a $P < 0.05$ in both biological replicates are highlighted in green. Proteins were considered concordantly regulated when changes in their expression levels followed the same trend in all treated samples across two independent experiments. The names of six concordantly regulated proteins are indicated. The intensities on the x-axis and the ratios on the y-axis are plotted on a Ln scale. The first of two biological replicates (E1) is shown. (C) Analysis of the TCGA skin cutaneous melanoma tumor dataset for the six genes from B. Table of gene-specific alteration frequencies of single or combined copy-number alterations, mutations, changes in mRNA expression or (phospho)protein levels detected by RPPA in all melanoma and different subgroups (BRAF mutant (MT), NRAS mutant (MT), BRAF/NRAS double mutant (MT), or BRAF/NRAS wild type (WT)).

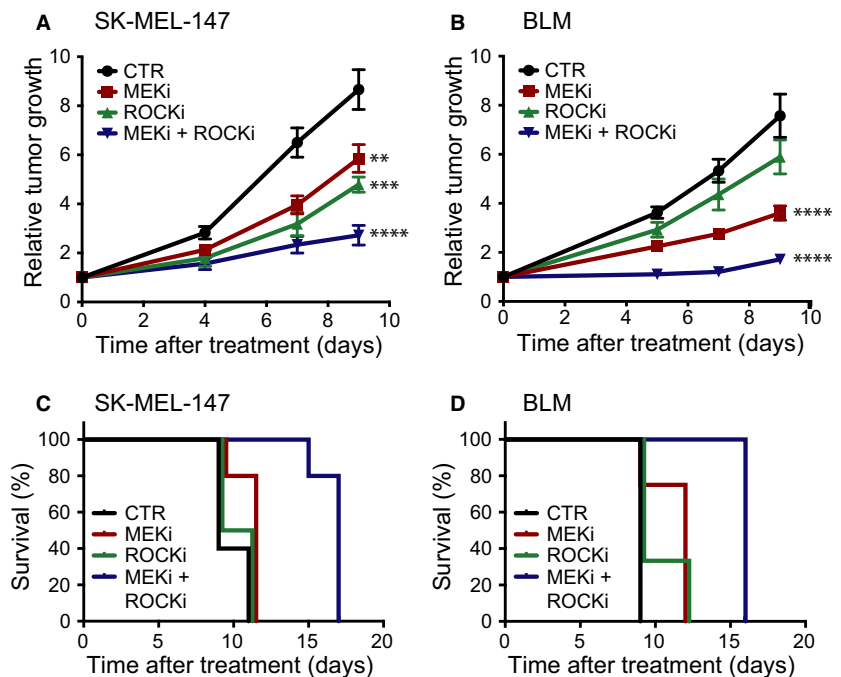
together with mice from the control group due to tumor burden. In contrast, the combination treatment prolonged the survival time significantly (Figure 4C). These findings were reproduced in an independent NRAS mutant melanoma cell line (BLM, Figure 4B,D). Plasma levels of GSK269962A in mice have not been reported before. We measured GSK269962A concentrations of 0.3–1.1 μ M (Table S5), indicating that the levels we used for in vitro experiments could be reached in vivo. In conclusion, combination of ROCK and MEK inhibitors significantly prolongs survival of mice carrying NRAS mutant melanomas.

Discussion

The identification of effective inhibitor combinations for NRAS mutant melanoma is challenging. Importantly, a recent combinatorial drug screening approach has revealed many more interactions between pairs of inhibitors for BRAF mutant melanoma than for NRAS

mutant or wild-type melanoma (Held et al., 2013). Among the few combination therapies proposed so far, combinations of MEK and PI₃K pathway inhibitors suppressed tumor growth of xenografted NRAS mutant melanoma cell lines more strongly than single agents (Posch et al., 2013), and a small molecule cotargeting the PI₃K and NF- κ B pathways inhibited the growth of grafted NRAS mutant and of BRAF mutant melanoma cells (Feng et al., 2011). Furthermore, a combination of a CDK4/6 and a MEK inhibitor for NRAS mutant melanoma is currently in phase Ib/II of clinical testing (Sosman et al., 2014). Targeting BRAF mutant melanoma with combinations of inhibitors such as BRAF and MEK inhibitors is more effective than treatment with single agents (Robert et al., 2015) and has been approved by the FDA in the USA. A similar strategy of targeting several components of the MAPK/ERK pathway, namely MEK and ERK, was reported recently for NRAS mutant melanoma, but has not been tested in vivo yet (Rebecca et al., 2014).

Figure 4. NRAS mutant melanoma is sensitive to the combined inhibition of MEK and ROCK in vivo. 5×10^5 melanoma cells [SK-MEL-147 (A, C) or BLM (B, D)] were subcutaneously injected into both flanks of NOD/SCID mice. After the tumors reached a volume of up to 150 mm³, mice received vehicle controls (CTR), MEKi (0.05 mg/kg, A, C, or 0.1 mg/kg, B, D), ROCKi GSK269962A (10 mg/kg), or both drugs by daily oral gavage. A, C: $n = 10$ tumors for each group except for ROCKi ($n = 8$). B, D: $n = 8$ tumors for each group except for ROCKi ($n = 6$). A, B show relative tumor growth. Error bars represent the SEM. P values comparing the control treated group to each of the treated groups individually: **: <0.01, ***: <0.001, ****: <0.0001. C, D show the corresponding Kaplan–Meier survival curves. Mice were euthanized when one of the tumors reached a volume of 1 cm³.



We present here an unanticipated possible alternative: a combination of either MEK or ERK inhibitor with ROCK inhibitor for NRAS mutant melanomas, which are treatment naïve. We show that nine of ten cell lines examined show cooperative induction of cell death upon the combination treatment (Figures 1A–E and 2, Figure S1). Also *in vivo*, we observed a significant tumor delay upon cotreatment with ROCK and MEK inhibitors (Figure 4). Importantly, also cells with acquired ERK inhibitor resistance were efficiently killed by this combinatorial treatment (Figure 1F and Figure S2A). Therefore, we propose that it will be worth exploring whether patients who develop resistance to currently used targeted therapies can benefit from switching to the one demonstrated here. Another advantage is that the addition of the ROCK inhibitor to the MEK inhibitor treatment allowed us to use very low doses of the MEK inhibitor. This is an important benefit, as serious dose-limiting on-target toxicities have been described for MEK inhibitors, which have forced patients with melanoma to stop treatment or lower the dose in spite of tumor control (Ascierto et al., 2013). We used low doses of the MEK inhibitor to clearly see the combination effect with the ROCK inhibitor. Therefore, decreasing the MEK inhibitor dosage or further improving ROCK inhibitors like GSK269962A, whose *in vivo* use and antitumor efficacy we demonstrate for the first time, may allow for more durable responses. Fasudil is well tolerated without any serious adverse reactions, and several clinical trials for diverse conditions have been performed or are currently recruiting patients in the United States (www.clinicaltrials.gov). It may therefore be explored for repurposing for the treatment of NRAS mutant melanomas in combination with a MEK inhibitor. Although we have focused here on primary tumor growth, ROCK inhibitors could have a beneficial effect on both primary tumor growth and metastatic spread (Nakajima et al., 2003). In particular, activated ROCK2 positively regulates cancer cell dissemination into the stroma and tumor angiogenesis in mice (Croft et al., 2004). As an added benefit, targeted therapies like the one proposed here could trigger the release of antigens, which might improve immunotherapy results (Frederick et al., 2013).

In addition to our *in vitro* and *in vivo* studies, our proteomics analyses identified a set of six proteins whose levels are concordantly changed in SK-MEL-147 cells by single treatment with MEK or ROCK inhibitors and which are more strongly changed by the combination treatment. Three of them are downregulated by the treatments: the GTPase-activating protein RACGAP1, the ubiquitin conjugating enzyme UBE2T, and ubiquitin ligase UHRF1 (Figure 3B). Increased levels of these factors (RACGAP1, UBE2T, UHRF1) are associated with several cancer types, including lung, breast, and gastric cancer (Liang et al., 2013; Ueki et al., 2009; Zhou et al., 2013) and with advanced stage, metastasis, and poor prognosis in colorectal cancer for RACGAP1 (Imaoka

et al., 2015) and in gastric cancer for UHRF1 (Zhou et al., 2013). They are also required for proliferation: RACGAP1 for cytokinesis (Matthews et al., 2012) and UBE2T and UHRF1 for G1/S progression (Arima et al., 2004; Machida et al., 2006). Downregulation of UBE2T and UHRF1 is associated with positive therapy response and tumor suppressor gene (re)expression (Alhosin et al., 2011; Ueki et al., 2009). The detected downregulation of RACGAP1, UBE2T, and UHRF1 upon MEK and ROCK inhibition correlates with the effectiveness of the treatment. The six corresponding genes are altered in melanoma and other cancers (Figure S6); they are affected somewhat more frequently in NRAS mutant and BRAF/NRAS double mutant melanomas than in BRAF mutant melanomas (Figure 3C). Furthermore, a recent study in non-melanoma cancer cell lines with NRAS^{Q61} mutations identified common dependencies on the MEK/ERK and other pathways (Vujic et al., 2014). Taken together, this suggests that our findings are applicable to NRAS mutant melanoma, although we have recently shown by integrated shRNA screening and proteomic analysis that the MEK/ROCK pathway co-inhibition is also effective in the BRAF setting (Smit et al., 2014).

In conclusion, we found an unexpected effect of combining MAPK/ERK pathway inhibitors with ROCK inhibitors on the induction of apoptotic and cytostatic responses of NRAS melanoma cells *in vitro* and suppression of tumor growth *in vivo*. Although this treatment would have to be optimized for clinical use, it will be worth exploring as patients carrying NRAS mutant melanomas currently have limited treatment options.

Methods

Inhibitors

MEK inhibitor GSK1120212/Trametinib, ROCK inhibitor Fasudil, BRAF inhibitor PLX-4720 were bought from Selleck Chemicals, Houston, TX, USA. ERK inhibitor SCH772984 was provided by Merck & Co, Whitehouse Station, NJ, USA (via a MTA). ROCK inhibitor GSK269962A was from Axon Medchem, Groningen, the Netherlands. Metabolic poison phenyl arsine oxide (PAO) and vehicle dimethylsulfoxide (DMSO) were from Sigma-Aldrich, St. Louis, MO, USA.

Cell lines, culture conditions, and inhibitor concentrations

Cell line sources: Mel 01.12, Mel 02.02, Mel 90.07, Mel 99.08 were from the Leiden University Medical Center, the Netherlands. BLM, FM6, MZ2-MEL, SK-MEL-2, SK-MEL-147 were acquired from within the NKI-AvL. WM1366 was from the Wistar Institute, USA (M. Herlyn). Cell line identity was verified with STR profiling where applicable (PowerPlex 16 HS; Promega, Leiden, The Netherlands). NRAS mutation status: Q61K (FM6, MZ2-MEL, Mel 02.02), Q61L (WM1366), Q61R (BLM, Mel 01.12, Mel 90.07, Mel 99.08, SK-MEL-2, SK-MEL-147). NRAS exon 3 and BRAF exon 15 were PCR amplified from genomic DNA and subjected to Sanger sequencing (Vredevelde et al., 2012). All cell lines were cultured in Dulbecco's modified Eagle's Medium (DMEM, Gibco (Life Technologies),

Blaiswijk, the Netherlands) supplemented with 9% fetal calf serum (Sigma-Aldrich) and 2 mM glutamine (Gibco). To generate ERKi-resistant sublines cells were plated on 10 cm dishes. Medium containing 1 μ M ERKi was added the next day and changed twice a week. After 2 weeks pools were generated by trypsinization and expanded in the presence of the inhibitor. All assays were performed with cell line-specific cell numbers and inhibitor concentrations (Table S6). Inhibitors were added 1 day after setup. Short-term viability assays were performed in 96-well plates with a dilution range of one inhibitor with or without a fixed concentration of a second inhibitor for 3 days. Then the medium was replaced by a 1:20 dilution of CellTiter Blue reagent (Promega) in full medium and fluorescence determined with an EnVision multilabel reader (Perkin Elmer, Waltham, MA, USA) or Infinite M200 microplate reader (Tecan, Giessen, Germany) after 2 h. Cell viability values were normalized to vehicle control DMSO-treated cells set to 100% and killing control PAO-treated cells set to 0% for each experiment. Each independent experiment (i.e. biological replicate) was performed as technical replicate in duplicates or triplicates. Curves were calculated as average values of at least three independent experiments as nonlinear curve fit with Prism version 6.0d (GraphPad Software, La Jolla, CA, USA). Long-term viability assays were performed in 6-well format. Inhibitor solutions were replaced every three to 4 days and plates stained with crystal violet after 7 days of treatment. For immunoblot analysis cells were treated on 10 cm dishes, both adherent and floating cells were collected and snap-frozen after harvesting.

Immunoblot analysis and antibodies

Cell pellets were lysed in RIPA buffer (50 mM TRIS pH 8.0, 150 mM NaCl, 1% Nonidet P-40, 0.5% sodium deoxycholate, 0.1% SDS, 1:25 diluted Roche complete protease inhibitor cocktail (Roche Applied Science, Almere, The Netherlands) and phosphatase inhibitors 10 mM NaF, 1 mM Na₃VO₄, 1 mM sodium pyrophosphate, 10 mM beta-glycerophosphate were added before use), lysates were cleared by centrifugation and protein concentration was determined with the Bio-Rad Protein Assay (Veenendaal, the Netherlands). Immunoblot analysis was performed with standard techniques using 4–12% Bis-Tris polyacrylamide-SDS gels (NuPAGE, Life Technologies) wet blotted onto nitrocellulose membranes (Whatman, GE Healthcare, Diegem, Belgium). Blots were blocked in 4% skimmed milk powder in PBS plus 0.2% Tween100 and incubated with primary antibodies: BD Transduction Laboratories, Franklin Lakes, NJ, USA: p27 (610241), ROCK1 (#611137); Bethyl Laboratories, Montgomery, TX, USA: ROCK2 (A300-047A); Cell Signaling Technology, Danvers, MA, USA: phospho-AKT1/2/3 (AKT1 Ser473, AKT2 Ser474, AKT3 Ser472 #9271), Bax (D2E11, #5023), Bik (#4952), Bim (C34C5, #2933), cleaved caspase 3 (Asp175, #9661), ERK1/2 (#9102), phospho-ERK1/2 (ERK1 Thr202/Tyr204, ERK2 Thr185/Tyr187, E10, #9106), MEK1/2 (L38C12, #4694), phospho-MEK1/2 (Ser217/221, 41G9, #9154), mTOR (7C10, #2983), phospho-mTOR (Ser2448, D9C2, #5536), p90RSK1/2/3 (p90) (32D7, #9355), PARP (#9542), Puma (#4976), RPS6 (5G10, #2217), phospho-RPS6 (Ser235/236, 2F9, #4856), phospho-RPS6 (Ser240/4, #2215); Merck Millipore, Billerica, MA, USA: phospho-p90RSK1 (Thr359/Ser363, #04-419); Santa Cruz, Dallas, TX, USA: AKT1/2/3 (sc-8312), Bcl-2 (N19, sc-492), Cyclin D1 (H295, sc-753), p16 (sc-56330, JC8), p21 (sc-397); Sigma-Aldrich: alpha-tubulin (DM 1A). Antibody signals from fluorescence-labeled secondary antibodies were detected with the Odyssey reader and software V3.0 (Li-Cor Biosciences, Lincoln, NE, USA).

ROCK kinase activity assay

The assay was performed with a modified protocol for the lysis buffer and kinase assay (Chun et al., 2011). Cells were treated as

for immunoblotting, both adherent and floating cells were collected and lysed in NP40 buffer (20 mM HEPES pH 7.4, 175 mM NaCl, 0.7% Nonidet NP-40, 10 mM EDTA, 1:25 diluted Roche complete protease inhibitor cocktail and phosphatase inhibitors 10 mM NaF, 1 mM Na₃VO₄, 1 mM sodium pyrophosphate, 10 mM beta-glycerophosphate were added before use). Five-hundred microgram protein at 1–2 μ g/ μ l was precleared with sepharose G beads (Amersham, Diegem, Belgium) for 30 min, incubated with 1 μ g ROCK2 antibody (A300-047A, Bethyl Laboratories) for 1 h and immunoprecipitated with sepharose G beads overnight. The beads were washed three times with 0.5 ml kinase buffer (20 mM Tris-HCl pH 7.5, 100 mM KCl₂, 5 mM MgCl₂, 5 mM MnCl₂, with 0.1 mM DTT, 2 mM EDTA added before use) and incubated with 40 μ l kinase buffer with 0.1% beta-mercaptoethanol, 100 μ M ATP, and 1 μ g recombinant human MYPT1 (Merck Millipore) at 30°C under agitation for 30 min. The reaction was stopped by boiling the samples in 20 μ l SDS sample buffer with beta-mercaptoethanol. Immunoblotting was performed as described above. 25 μ g lysate as input controls and 20 μ l of the kinase reaction volume were used to detect ROCK2 kinase activity. ROCK1 (611137, BD Transduction Laboratories, Franklin Lakes, NJ, USA), ROCK2 (A300-047A, Bethyl Laboratories, Montgomery, TX, USA), alpha-tubulin (Sigma-Aldrich), and MYPT1 phosphorylation at Thr696 (ABS45; Merck Millipore) were detected and quantified on the same membrane with the Odyssey reader. ROCK2 kinase activity was normalized to ROCK2 abundance per sample and to baseline activity in untreated cells.

In vivo assays

Six- to ten-week-old male NOD/SCID mice were injected subcutaneously with 5×10^5 cells in growth factor-reduced matrigel (Becton Dickinson, Franklin Lakes, NJ, USA) into both flanks. When the tumors reached a volume of up to 150 mm³, mice were randomized to ensure an equal tumor volume distribution per group. Mice were treated by daily oral gavage with MEKi (GSK1120212/Trametinib, 0.05–0.1 mg/kg, in 5% Tween 80, 3.25% ethanol, 2–4% DMSO), ROCKi (GSK266962A, 10 mg/kg, in 10% Tween 80, 6.5% ethanol, 5–10% DMSO), both inhibitors, or vehicle control (10% Tween 80, 6.5% ethanol, 5–10% DMSO). Twice a week tumor sizes were measured with a caliper and body weight was determined. Tumor volume was calculated by the formula $(a \times b^2)/2$, with 'a' being the longest diameter and 'b' the respective perpendicular diameter of the tumor. Mice were euthanized with CO₂ when one of the tumors reached a volume of 1 cm³, according to the protocol approved by the Institutional Animal Experiment Ethics Committee. Significance was calculated with an ordinary one-way ANOVA test, corrected for multiple comparisons with Dunnett's test. ROCKi GSK266962A concentrations in heparin plasma were measured using a reversed-phase LC-electrospray MS/MS method in the range 10–10 000 nM with PLX-4720 as internal standard (for a detailed description see Data S1).

Proteomic mass spectrometry analysis

Sample preparation, mass spectrometry analysis, and data analysis with DAVID are described in the Data S1. The mass spectrometry proteomics data have been deposited to the ProteomeXchange Consortium (<http://proteomecentral.proteomexchange.org>) via the PRIDE partner repository (Vizcaino et al., 2012) with the dataset identifier PXD000528. ProteomeXchange submission title: Melanoma NRAS. ProteomeXchange accession: PXD000528.

Genetic analysis of cancer datasets

The analyses are described in the Data S1.

Acknowledgements

We would like to thank S. Greven, M. Voetel, H. Grimminck, S. de Jong, and A. Shahrabai for excellent technical help with in vivo experiments and the animal pathology department, J.Y. Song and S. Klarenbeek for help with the pathological analysis. We thank S. Douma for excellent technical assistance, all members of the Peeper laboratory for their valuable input, S. Durmus, A. H. Schinkel, and A. Hooijkaas for advice on the in vivo administration of the inhibitors, and Merck for financial support and for providing ERK inhibitor SCH772984. This work was supported by the Deutsche Forschungsgemeinschaft, Germany (Research Fellowship, C.J.V.), Vetenskapsrådet (VR), Sweden (International Postdoc grant, G.M.), The Netherlands Proteomics Center, embedded in The Netherlands Genomics Initiative, the Netherlands Organization for Scientific Research (NWO) with a VIDI grant to A.F.M.A, a Queen Wilhelmina award and a grant from the Dutch Cancer Society (KWF) (M.A.S., P.A.P., D.S.P.).

Conflict of interest

A patent for the combination of MEK and ROCK inhibitors for the treatment of NRAS mutant melanoma has been filed with C.J.V., M.A.S., and D.S.P. as inventors.

References

- Alhosin, M., Sharif, T., Mousli, M., Etienne-Selloum, N., Fuhrmann, G., Schini-Kerth, V.B., and Bronner, C. (2011). Down-regulation of UHRF1, associated with re-expression of tumor suppressor genes, is a common feature of natural compounds exhibiting anti-cancer properties. *J. Exp. Clin. Cancer Res.* *30*, 41.
- Alteelaar, A.F.M., Munoz, J., and Heck, A.J.R. (2013). Next-generation proteomics: towards an integrative view of proteome dynamics. *Nat. Rev. Gen.* *14*, 35–48.
- Amano, M., Nakayama, M., and Kaibuchi, K. (2010). Rho-kinase/ROCK: a key regulator of the cytoskeleton and cell polarity. *Cytoskeleton* *67*, 545–554.
- Arima, Y., Hirota, T., Bronner, C., Mousli, M., Fujiwara, T., Niwa, S., Ishikawa, H., and Saya, H. (2004). Down-regulation of nuclear protein ICBP90 by p53/p21Cip1/WAF1-dependent DNA-damage checkpoint signals contributes to cell cycle arrest at G1/S transition. *Genes Cells* *9*, 131–142.
- Aronov, A.M., Tang, Q., Martinez-Botella, G. et al. (2009). Structure-guided design of potent and selective pyrimidopyrrole inhibitors of extracellular signal-regulated kinase (ERK) using conformational control. *J. Med. Chem.* *52*, 6362–6368.
- Ascierto, P.A., Schadendorf, P.D., Berking, C. et al. (2013). MEK162 for patients with advanced melanoma harbouring. *Lancet Oncol.* *14*, 249–256.
- Chapman, P.B., Hauschild, A., Robert, C. et al. (2011). Improved survival with vemurafenib in melanoma with BRAF V600E mutation. *N. Engl. J. Med.* *364*, 2507–2516.
- Chun, K.H., Choi, K.D., Lee, D.H., Jung, Y., Henry, R.R., Ciaraldi, T.P., and Kim, Y.B. (2011). In vivo activation of ROCK1 by insulin is impaired in skeletal muscle of humans with type 2 diabetes. *Am. J. Physiol. Endocrinol. Metab.* *300*, E536–E542.
- Croft, D.R., Sahai, E., Mavria, G., Li, S., Tsai, J., Lee, W.M.F., Marshall, C.J., and Olson, M.F. (2004). Conditional ROCK activation in vivo induces tumor cell dissemination and angiogenesis. *Cancer Res.* *64*, 8994–9001.
- Diaz, L.A., Williams, R.T., Wu, J. et al. (2012). The molecular evolution of acquired resistance to targeted EGFR blockade in colorectal cancers. *Nature* *486*, 537–540.
- Dry, J.R., Pavey, S., Pratilas, C.A. et al. (2010). Transcriptional pathway signatures predict MEK addiction and response to selumetinib (AZD6244). *Cancer Res.* *70*, 2264–2273.
- Eggermont, A.M., Spatz, A., and Robert, C. (2014). Cutaneous melanoma. *Lancet* *383*, 816–827.
- Fedorenko, I.V., Gibney, G.T., and Smalley, K.S.M. (2013). NRAS mutant melanoma: biological behavior and future strategies for therapeutic management. *Oncogene* *32*, 3009–3018.
- Feng, Y., Barile, E., De, S.K. et al. (2011). Effective inhibition of melanoma by BI-69A11 is mediated by dual targeting of the AKT and NF- κ B pathways. *Pigment Cell Melanoma Res.* *24*, 703–713.
- Frederick, D.T., Piris, A., Cogdill, A.P. et al. (2013). BRAF inhibition is associated with enhanced melanoma antigen expression and a more favorable tumor microenvironment in patients with metastatic melanoma. *Clin. Cancer Res.* *19*, 1225–1231.
- Gilmartin, A.G., Bleam, M.R., Groy, A. et al. (2011). GSK1120212 (JTP-74057) is an inhibitor of MEK activity and activation with favorable pharmacokinetic properties for sustained in vivo pathway inhibition. *Clin. Cancer Res.* *17*, 989–1000.
- Hauschild, A., Grob, J.-J., Demidov, L.V. et al. (2012). Dabrafenib in BRAF-mutated metastatic melanoma: a multicentre, open-label, phase 3 randomised controlled trial. *Lancet* *380*, 358–365.
- Held, M.A., Langdon, C.G., Platt, J.T. et al. (2013). Genotype-selective combination therapies for melanoma identified by high-throughput drug screening. *Cancer Discov.* *3*, 52–67.
- Imaoka, H., Toiyama, Y., Saigusa, S. et al. (2015). RacGAP1 expression, increasing tumor malignant potential, as a predictive biomarker for lymph node metastasis and poor prognosis in colorectal cancer. *Carcinogenesis* *36*, 346–354.
- Ji, Z., Flaherty, K.T., and Tsao, H. (2012). Targeting the RAS pathway in melanoma. *Trends Mol. Med.* *18*, 27–35.
- Karnoub, A.E., and Weinberg, R.A. (2008). Ras oncogenes: split personalities. *Nat. Rev. Mol. Cell Biol.* *9*, 517–531.
- Liang, Y., Liu, M., Wang, P., Ding, X., and Cao, Y. (2013). Analysis of 20 genes at chromosome band 12q13: RACGAP1 and MCRS1 overexpression in non-small-cell lung cancer. *Genes Chromosom. Cancer* *52*, 305–315.
- Machida, Y.J., Machida, Y., Chen, Y., Gurtan, A.M., Kupfer, G.M., D'Andrea, A.D., and Dutta, A. (2006). UBE2T is the E2 in the Fanconi anemia pathway and undergoes negative autoregulation. *Mol. Cell* *23*, 589–596.
- Matthews, H.K., Delabre, U., Rohn, J.L., Guck, J., Kunda, P., and Baum, B. (2012). Changes in Ect2 localization couple actomyosin-dependent cell shape changes to mitotic progression. *Dev. Cell* *23*, 371–383.
- Mendoza, M.C., Er, E.E., and Blenis, J. (2011). The Ras-ERK and PI3K-mTOR pathways: cross-talk and compensation. *Trends Biochem. Sci.* *36*, 320–328.
- Morris, E.J., Jha, S., Restaino, C.R. et al. (2013). Discovery of a novel ERK inhibitor with activity in models of acquired resistance to BRAF and MEK inhibitors. *Cancer Discov.* *3*, 742–750.
- Nakajima, M., Hayashi, K., Egi, Y. et al. (2003). Effect of Wf-536, a novel ROCK inhibitor, against metastasis of B16 melanoma. *Cancer Chemother. Pharmacol.* *52*, 319–324.
- Ostrem, J.M., Peters, U., Sos, M.L., Wells, J.A., and Shokat, K.M. (2014). K-Ras(G12C) inhibitors allosterically control GTP affinity and effector interactions. *Nature* *503*, 548–551.
- Packer, L.M., East, P., Reis-Filho, J.S., and Marais, R. (2009). Identification of direct transcriptional targets of (V600E)BRAF/MEK signalling in melanoma. *Pigment Cell Melanoma Res.* *22*, 785–798.
- Patel, R.A., Forinash, K.D., Pireddu, R., Sun, Y., Sun, N., Martin, M.P., Schonbrunn, E., Lawrence, N.J., and Sebt, S.M. (2012). RKI-1447 is a potent inhibitor of the Rho-associated ROCK kinases with

- anti-invasive and antitumor activities in breast cancer. *Cancer Res.* 72, 5025–5034.
- Posch, C., Moslehi, H., Feeney, L. et al. (2013). Combined targeting of MEK and PI3K/mTOR effector pathways is necessary to effectively inhibit NRAS mutant melanoma in vitro and in vivo. *Proc. Natl Acad. Sci. USA* 110, 4015–4020.
- Rath, N., and Olson, M.F. (2012). Rho-associated kinases in tumorigenesis: re-considering ROCK inhibition for cancer therapy. *EMBO Rep.* 13, 900–908.
- Rebecca, V.W., Alicea, G.M., Paraiso, K.H.T., Lawrence, H., Gibney, G.T., and Smalley, K.S.M. (2014). Vertical inhibition of the MAPK pathway enhances therapeutic responses in NRAS-mutant melanoma. *Pigment Cell Melanoma Res.* 27, 1154–1158.
- Robert, C., Karaszewska, B., Schachter, J. et al. (2015). Improved overall survival in melanoma with combined dabrafenib and trametinib. *N. Engl. J. Med.* 372, 30–39.
- Routhier, A., Astuccio, M., Lahey, D. et al. (2010). Pharmacological inhibition of Rho-kinase signaling with Y-27632 blocks melanoma tumor growth. *Oncol. Rep.* 23, 861–867.
- Sahai, E., Olson, M.F., and Marshall, C.J. (2001). Cross-talk between Ras and Rho signalling pathways in transformation favours proliferation and increased motility. *EMBO J.* 20, 755–766.
- Sebbagh, M., Renvoize, C., Hamelin, J., Riche, N., Bertoglio, J., and Breard, J. (2001). Caspase-3-mediated cleavage of ROCK I induces MLC phosphorylation and apoptotic membrane blebbing. *Nat. Cell Biol.* 3, 346–352.
- Smit, M.A., Maddalo, G., Greig, K., Raaijmakers, L.M., Possik, P.A., van Breukelen, B., Cappadona, S., Heck, A.J., and Altelaar, A.M., Peeper, D.S. (2014). ROCK1 is a potential combinatorial drug target for BRAF mutant melanoma. *Mol. Syst. Biol.* 10, 772.
- Sosman, J.A., Kittaneh, M., Lolkema, M.P.J.K., Postow, M.A., Schwartz, G., Franklin, C., Matano, A., Bhansali, S., Parasuraman, S., and Kim, K. (2014). A phase 1b/2 study of LEE011 in combination with binimetinib (MEK162) in patients with NRAS-mutant melanoma: early encouraging clinical activity. *ASCO Meet. Abstr.* 32, 9009.
- Street, C.A., and Bryan, B.A. (2011). Rho Kinase Proteins—Pleiotropic modulators of cell survival and apoptosis. *Anticancer Res.* 31, 3645–3658.
- Ueki, T., Park, J.-H., Nishidate, T., Kijima, K., Hirata, K., Nakamura, Y., and Katagiri, T. (2009). Ubiquitination and downregulation of BRCA1 by ubiquitin-conjugating enzyme E2T overexpression in human breast cancer cells. *Cancer Res.* 69, 8752–8760.
- Vizcaino, J.A., Cote, R.G., Csordas, A. et al. (2012). The Proteomics Identifications (PRIDE) database and associated tools: status in 2013. *Nucleic Acids Res.* 41, D1063–D1069.
- Vredevelde, L.C.W., Possik, P.A., Smit, M.A. et al. (2012). Abrogation of BRAFV600E-induced senescence by PI3K pathway activation contributes to melanomagenesis. *Genes Dev.* 26, 1055–1069.
- Vujic, I., Posch, C., Sanlorenzo, M. et al. (2014). Mutant NRASQ61 shares signaling similarities across various cancer types—potential implications for future therapies. *Oncotarget* 5, 7936–7944.
- Walia, V., Mu, E.W., Lin, J.C., and Samuels, Y. (2012). Delving into somatic variation in sporadic melanoma. *Pigment Cell Melanoma Res.* 25, 155–170.
- Zhou, L., Zhao, X., Han, Y., Lu, Y., Shang, Y., Liu, C., Li, T., Jin, Z., Fan, D., and Wu, K. (2013). Regulation of UHRF1 by miR-146a/b modulates gastric cancer invasion and metastasis. *FASEB J.* 27, 4929–4939.

Supporting information

Additional Supporting Information may be found in the online version of this article:

Figure S1. Treatment-naïve NRAS mutant melanoma cells are sensitive to combinatorial inhibition of MAPK/ERK and ROCK pathways.

Figure S2. ERK inhibitor-resistant NRAS mutant melanoma cells are sensitive to combinatorial inhibition of MAPK/ERK and ROCK pathways.

Figure S3. ROCK and MEK or ERK inhibitors cooperatively induce apoptosis.

Figure S4. ROCK and MEK or ERK inhibitors cooperatively induce apoptosis in adherent cells.

Figure S5. ROCK and MEK inhibitors cooperatively alter the proteome.

Figure S6. Cross cancer distribution of genetic alterations of proteins regulated upon MEK and ROCK inhibitor treatment.

Table S1. Proteomic mass spectrometry analyses of MEK and ROCK inhibitor treated melanoma cells.

Table S2. Pathway analysis of proteomics data from MEK and ROCK inhibitor treated melanoma cells.

Table S3. Gene set alteration frequencies per gene in melanoma.

Table S4. Gene set alteration frequencies across cancer types.

Table S5. Plasma levels of ROCK inhibitor GSK269962A in mice.

Table S6. Cell numbers and inhibitor concentrations.

Data S1. Materials and Methods.